Suppression of superconductor quasiparticle tunneling into single-walled carbon nanotubes

V. Krstić[1,2,*] S. Roth,[1] M. Burghard,[1] J. Weis,[1] and K. Kern[1]
[1]*Max-Planck-Institut für Festkörperforschung, Heisenbergstr. 1, D-70569 Stuttgart, Germany*
[2]*Grenoble High Magnetic Field Laboratory, Max-Planck-Institut für Festkörperforschung/CNRS, B.P. 166, F-38042 Grenoble, France*
(Received 10 July 2002; published 3 November 2003)

Electrical transport through single-walled carbon nanotubes with weak electrical coupling to superconducting leads has been studied theoretically and experimentally. A simple model is considered to describe single-particle tunneling into a Luttinger-liquid-like state from electrically weak connected superconducting electrodes. This involves the superconductor's quasiparticle and the Luttinger liquid's excitation density of states. Experimentally, the suppression of quasiparticle tunneling induced current peaks was observed at temperatures below 0.1 K, which we attributed to the Luttinger-liquid-like excitation spectrum of the single-walled carbon nanotube.

DOI: 10.1103/PhysRevB.68.205402 PACS number(s): 73.63.−b, 73.22.Lp

Single-electron charging was one of the first effects observed and investigated in electrical transport in single-walled carbon nanotubes (SWNTs).[1,2] In these works it was demonstrated that SWNTs weakly connected to metal electrodes can be used as molecular transistors,[2] and that transport spectroscopy provides a first insight into the electronic excitation spectrum of SWNTs. The experimental data have been interpreted in the framework of the constant interaction model.[3] In particular, visible excitations were attributed to quantization effects due to the finite length of the SWNTs under investigation.

However, for the majority of results on transport spectroscopy, it has been apparent that the excitation spectrum of the SWNTs is much more complex than predicted by the constant interaction model. It is assumed that the deviations originate from the strong one-dimensional character of the SWNTs. This is supported by the experimental observation that SWNTs with strong electrical connections to metal leads exhibit signatures of electron-electron correlations in their current/voltage (I/V_{sd}) characteristics at low temperatures.[4] The electron system of the SWNT was described as a Luttinger-liquid (LL) state where the basic charged excitation is a propagating soundlike excitation (plasmon).[5] In multiwalled carbon nanotubes a LL-like behavior has also been found, observed in the form of the so-called zero-bias anomaly in conductance measurements.[6]

In the present work, a simple, qualitative model is presented which describes electrical transport through a LL, and therefore also through a SWNT, with a weak electrical coupling to superconducting electrodes. The qualitative predictions of the theoretical model are compared with experimental data on SWNTs weakly connected electrically to superconducting rhenium (Re) terminals.

In general, electrical transport through a physical object (or island) with weak electrical connection (roughly speaking, the contact resistance exceeds the quantum resistance $h/e^2 \approx 25.8\,\mathrm{k}\Omega$) to BCS superconductor leads occurs through quasiparticle (QP) tunneling. In contrast, for lower contact resistances, the proximity effect is apparent as observed for SWNTs in Ref. 7. QPs are the single-particle excitations of the superconducting ground state and behave generally similarly to electrons. Before discussing the QP tunneling process and thus the stationary current through the system, it is worthwhile to look at the energetic situation of the system when a finite source-drain voltage $V_{\mathrm{sd}}=(\mu_s-\mu_d)/e$ is applied at some fixed gate voltage V_g, as depicted in Fig. 1(a). As the reservoirs are superconducting, the temperature-dependent superconductor gap $2\Delta(T)$ separates the occupied (shaded) from the unoccupied QP energy levels. The QP density of states $D_{\mathrm{QP}}(\varepsilon)$ is of the form

$$D_{\mathrm{QP}}(\varepsilon) \propto \frac{|\varepsilon|}{\sqrt{\varepsilon^2-\Delta^2(T)}} \quad \text{for } |\varepsilon|>\Delta(T), \tag{1}$$

and zero for $|\varepsilon| \leqslant \Delta(T)$, and is also indicated in Fig. 1(a). Note that, ε is measured relative to the electrochemical potential of the BCS superconductor reservoirs and can be either positive or negative.

In between the reservoirs the relative position of the long beams denote the energy difference $\mu(n+1;\{V_l\}) \equiv E(n+1,0;\{V_l\}) - E(n,0;\{V_l\})$ between the two ground-state energies $E(n+1,0;\{V_l\})$ and $E(n,0;\{V_l\})$ of the $n+1$ and the n electron systems on the island, respectively, for the voltages $\{V_l\} \equiv \{V_g, V_{\mathrm{sd}}\}$.[8] The short beams are the corresponding energy differences $E(n+1,j;\{V_l\}) - E(n,i;\{V_l\}), i,j \geqslant 0$, for transitions to excited states of the electron system on the island. The indices i and j stand for a complete set of quantum numbers characterizing the state uniquely ($i=0$, $j=0$ for ground states). Without a loss of generality, in this figure, $2\Delta(T)$ is chosen to be smaller than the energy level distance $\mu(n+1;\{V_l\}) - \mu(n;\{V_l\})$. A tunneling event is indicated using the jth excited state of the $n+1$ electron system. From this energy scheme the expected transport regions within the (V_{sd} vs V_g) plane can be derived. This is shown in Fig. 1(b), using the general case of asymmetric capacitive couplings α_s and α_d of source- and drain electrodes, respectively.

If the energy difference between ground-states of adjacent electron number varies, as is usually the case for nonmetallic islands, the shape and size of the transport regions (diamonds) may differ from each other in contrast to the plot in

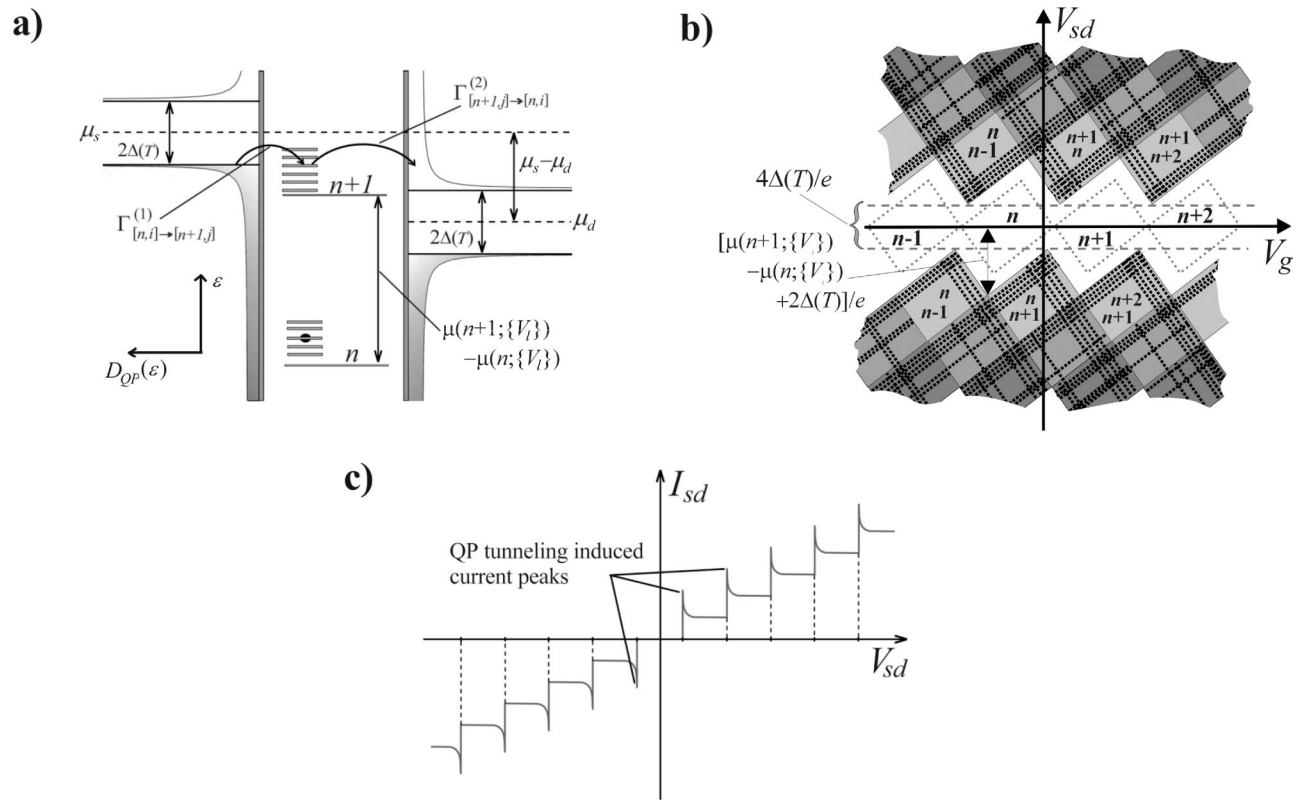

FIG. 1. (a) Energy scheme for a superconductor/island/superconductor arrangement at finite bias voltage. μ_s and μ_d are the electrochemical potentials of the superconducting reservoirs left and right, respectively. The shaded areas below the superconducting gap correspond to occupied QP states. Starting from n electrons on the island in the ground state, a tunneling process is indicated using the jth excited state of the $n+1$ electron system. The transition rates $\Gamma^{(1)}_{[n,i]\to[n+1,j]}$ and $\Gamma^{(2)}_{[n+1,j]\to[n,i]}$ for the tunneling process and the energy difference $\mu(n;\{V_l\})$ and $\mu(n+1;\{V_l\})$ are denoted. (b) In the ($V_{\rm sd}$ vs V_g)-plane, transport regions are derived from the energy scheme in (a), showing the familiar regular diamondlike pattern (gray colored) as known from systems exhibiting single-electron tunneling. White regions correspond to situations where no current is flowing through the island and the number of charges n on the island remains stable. Gray regions denote configurations of the system where current flow is enabled, i.e., the number of charges on the island fluctuates. The gray scale indicates the contribution of more possible charge states on the island to the current. For example the light gray regions fluctuate between two charge states of the island, e.g., n and $n+1$. The next darker region indicates fluctuations between three charge states, e.g., n, $n+1$, and $n+2$, and so forth. The solid black lines denote the onset of tunneling channels between ground-states of the island. The dotted lines in the gray regions indicate the onset from which excited states contribute to the electrical transport for sufficiently high bias voltages. In contrast to islands which are weakly connected electrically to normal metal electrodes a ''currentless band'' of the width $4\Delta(T)/e$ forms along the V_g axis. For comparison, additional diamonds (dotted line) in the white regions are shown which correspond to the case that normal metal leads would have been chosen for contacting the system. (c) $I/V_{\rm sd}$ characteristics of the SC/island/SC system. Peaks at each onset of a current step [solid lines in (b)] are apparent, originating from the QP density of states of the superconducting leads.

Fig. 1(b). As the QPs tunnel one after another through the island due to the weak electrical coupling, with increasing $|V_{\rm sd}|$ at fixed V_g, the current increases steplike when crossing a line in Fig. 1(b): a solid black line describes transitions between ground states of the $n+1$ and n electron systems, i.e., crossing a solid line energetically allows an additional charge state on the island. A dotted line gives an additional contribution to the current by excited states, either of the $n+1$ or n electron states. However, in contrast to islands which are connected to normal metal electrodes, for $|V_{\rm sd}|<2\Delta(T)/e$ no current can flow for any value of V_g. Along the V_g axis a ''currentless band'' of width $4\Delta(T)/e$ is formed.

For a more quantitative description of the electrical transport, first the transition rates of a tunneling event have to be determined from which the stationary current through the device can be derived. The transition rates depend on the following physical quantities: (i) changes in the total energy for rearranging electrons in the system as a tunnel event occurs under energy conservation, (ii) the matrix element $|t^{(r)}_{i\to j}(\varepsilon)|$ for the tunneling of a single QP with energy ε onto the island, and (iii) the number of QPs at a given energy ε which is given by the product of the QP density of states $D_{\rm QP}(\varepsilon)$ and the Fermi distribution $f(\varepsilon,\mu_r)$ (μ_r is the electrochemical potential of reservoir r).

The transition rate for QP tunneling from the superconducting reservoir r onto the island, inducing a transition from the island state $[n, i]$ to $[n+1,j]$ [also see Fig. 1(a)], is[9,10]

$$\Gamma^{(r)}_{[n,i]\to[n+1,j]} = \frac{2\pi}{\hbar}\int_{-\infty}^{\infty} |t^{(r)}_{i\to j}(\varepsilon)|^2 D_{\mathrm{QP}}(\varepsilon) f(\varepsilon,\mu_r) \times \delta[E(n+1,j;\{V_l\}) - E(n,i;\{V_l\}) - (\mu_r+\varepsilon)]\, d\varepsilon, \quad (2)$$

where the delta distribution $\delta(E(n+1,j;\{V_l\}) - E(n,i;\{V_l\}) - (\mu_r+\varepsilon))$ accounts for the energy conservation of the tunneling process. The stationary current through the island is directly proportional to $\Gamma^{(r)}_{[n,i]\to[n+1,j]}$,[9,10]

$$I_{\mathrm{stat}} = e\sum_n \sum_i \sum_j \{\Gamma^{(1)}_{[n,i]\to[n+1,j]} - \Gamma^{(2)}_{[n,i]\to[n+1,j]}\} P_{[n,i]}, \quad (3)$$

where the sums are over all charge states n of the island and over all excited states i and j of n and the $n+1$ electron systems on the island, respectively. $P_{[n,i]}$ is the probability of finding the island in the ith excited n-electron state for a given $\{V_l\}$. The latter is constrained by the condition $\Sigma_n \Sigma_i P_{[n,i]} = 1$, but this is not vital for the following discussion. Equation (3) can be simplified assuming that the system is, before each tunneling event, in the ground state of the respective electron number: in Eq. (3) the sum over i can be neglected except for the term with $i=0$. For a dense excitation spectrum it is more convenient to convert the sum over j into an integral form. For this, the density of states $\tau_{n+1}(\epsilon_{\mathrm{exc}})$ of the excitations of the $n+1$ state has to be introduced, transforming Eq. (2) to

$$\Gamma^{(r)}_{[n,0]\to[n+1,\epsilon_{\mathrm{exc}}]} = [\tau_{n+1}(\epsilon_{\mathrm{exc}})\, d\epsilon_{\mathrm{exc}}] \times \frac{2\pi}{\hbar}\int_{-\infty}^{\infty} |t^{(r)}(\varepsilon)|^2 D_{\mathrm{QP}}(\varepsilon)\cdot f(\varepsilon,\mu_r) \times \delta[\mu(n+1;\{V_l\}) + \epsilon_{\mathrm{exc}} - (\mu_r+\varepsilon)]\, d\varepsilon, \quad (4)$$

where the definition $E(n+1,\epsilon_{\mathrm{exc}};\{V_l\}) \equiv E(n+1,0;\{V_l\}) + \epsilon_{\mathrm{exc}}$ has been used and $\tau_{n+1}(\epsilon_{\mathrm{exc}})\, d\epsilon_{\mathrm{exc}}$ describes the degeneracy of the $n+1$ electron state at the excitation ϵ_{exc}. Carrying out the integral in Eq. (4) with the aid of the delta distribution, the transition rate is found to depend on the product $\tau_{n+1}(\epsilon_{\mathrm{exc}}) D_{\mathrm{QP}}[\mu(n+1;\{V_l\}) - \mu_r + \epsilon_{\mathrm{exc}}]$.

In the case of a metallic island at low temperatures, $\tau_{n+1}(\epsilon_{\mathrm{exc}})$ varies only slightly such that it can be assumed to be constant. Therefore the transition rate and thus I_{stat} is mainly determined by the dependence of $D_{\mathrm{QP}}(\varepsilon)$ on ε. Since $D_{\mathrm{QP}}(\varepsilon) \propto |\varepsilon|/\sqrt{\varepsilon^2 - \Delta^2(T)}$ for $|\varepsilon| > \Delta(T)$, I_{stat} is strongly enhanced for QP energies $|\varepsilon|$ close to $\Delta(T)$. In contrast, for $|\varepsilon| \gg \Delta(T)$, I_{stat} is smaller which leads to the formation of peaks at the onset of each step in the I/V_{sd} characteristics. This is caused by allowing an additional charge state on the island [see Fig. 1(c)]. This result is in agreement with experimental data on spherical metallic islands[11] and also coincides with other theoretical works[12] from which also the minor influence of $|t^{(r)}_{i\to j}(\varepsilon)|$ on the development of the current peaks is apparent.

In the case of a LL-like state $\tau_{n+1}(\epsilon_{\mathrm{exc}}) \sim \epsilon^{\gamma}_{\mathrm{exc}}$, also called tunneling density of states, can not be regarded as constant in contrast to a metallic system.[5] The exponent γ is a measure of the interaction strength and thus determines how strong the LL-like character is developed for a certain island. Therefore, the corresponding I_{stat} is determined by the dependence of the full product $\tau_{n+1}(\epsilon_{\mathrm{exc}}) D_{\mathrm{QP}}[\mu(n+1;\{V_l\}) - \mu_r + \epsilon_{\mathrm{exc}}]$ on ϵ_{exc}. For energies ϵ_{exc} close to zero, i.e., for lowest charged collective excitations (plasmons), $\tau_{n+1}(\epsilon_{\mathrm{exc}})$ is a decreasing and $D_{\mathrm{QP}}[\mu(n+1;\{V_l\}) - \mu_r + \epsilon_{\mathrm{exc}}]$ an increasing finite valued function. This has the effect that the high density of states of the QPs is counterbalanced by the vanishing tunneling density of states approaching the ground-state of the LL. Consequently, according to Eq. (3) the current at the onset of a current-step in the current/voltage-characteristics of this system is suppressed, at least in its height, in contrast to spherical metal islands.[11,12] Also, the simple model implies that at $\epsilon_{\mathrm{exc}} = 0$, which corresponds to tunneling into the ground-state of the $n+1$ electron system, the current is completely suppressed since $\tau_{n+1}(\epsilon_{\mathrm{exc}})$ vanishes. This is consistent with the fact that the basic charged excitation of a LL-like state is a plasmon mode in agreement with other theoretical considerations.[5]

As SWNTs are known to exhibit a LL-like behavior at low temperatures,[4] a weak electrical contacting of the tubes to superconducting electrodes should reveal, according to the considerations drawn above, a suppression of the current peaks at the onset of steps in the I/V_{sd} characteristics. In order to investigate whether SWNTs show this effect, SWNTs have been connected to superconducting leads from top. For this, SWNT raw material was first purified via centrifugation and then adsorbed[13] on a heavily doped Si wafer with a thermally grown SiO_2 layer (about 100 nm thick) which serves as a backgate. Electron-beam lithography was then used to generate a three-finger electrode pattern on top of the SWNTs, similar to Ref. 14. As electrode material, pure rhenium (Re) was chosen as it exhibits in thin films down to 50-nm thickness a critical temperature $T_c^{(\mathrm{film})}$ of about 6.7 K.[15] For this, the Re was evaporated on top of the SWNTs at liquid nitrogen temperature. Additionally, as the superconductor material is contacting the SWNTs from above, any contribution from bending defects is avoided.[17] In Fig. 2 a typical Re-electrode structure connecting a thin SWNT bundle ($\lesssim$3 nm in height) is shown. The inner electrode lines are 23 nm in height, 120 nm in width, and 2 μm in length. The distance between the electrode lines is about 200 nm. The schematic structure of the device is shown within the inset. The line from center right is continuous and contacted at both ends electrically in order to prove that the lines are still superconducting, despite their considerably reduced dimensions compared to thin films.[15] The room-temperature resistance of the continuous line was found to be about 10 kΩ which agrees with the estimated resistance of a Re bar of comparable dimensions using 17.2×10^{-8} Ωm for the Re resistivity.[16]

The room temperature two-point resistances for the electrode pairs (I), (II), and (III) are 1.7, 5.5, and 4.7 MΩ, respectively. These resistances indicate a contact resistance considerably higher than h/e^2, giving rise to single-electron

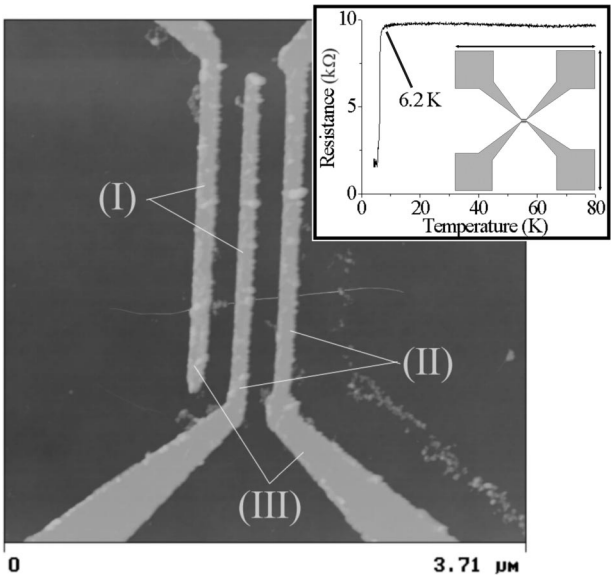

FIG. 2. Typical Re-electrode structure connecting a thin SWNT bundle ($\lesssim$3 nm in height). The distance between the inner electrode lines (2 μm in length) is about 200 nm. The height of the electrodes lines is 23 nm and their width is 120 nm. On the substrate some residuals from the fabrication process are observed, indicating that the Re is more ductile than Au or AuPd. Upper inset: temperature dependence of the resistance of the continuous line. At $T=6.2$ K a sharp drop is observed, indicative of the superconducting transition of the Re electrodes. In the inset a sketch of the Re-electrode pattern is shown. The size of the total pattern is 460×460 μm^2.

tunneling effects at sufficiently low temperatures.[1,2,18] The measurements have been performed in a ^{3}He/^{4}He-dilution refrigerator with a base temperature of 25 mK.

In the inset of Fig. 2 the temperature dependence of the resistance of the continuous line is plotted. At 6.2 K an abrupt decrease from its room-temperature value is observed. This significant reduction of the resistance at a temperature close to the critical temperature of thin films of Re clearly indicates that the electrode lines are indeed still superconducting in spite of their reduced geometrical dimensions. Remarkably, this temperature is close to $T_c^{(\mathrm{film})}$ and the superconductor energy gap at zero temperature can be deduced to be $2\Delta_0=3.5k_BT_c\approx1.8$ meV.[19]

In Fig. 3 the I/V_{sd} characteristics of the pair of electrodes (I), (II), and (III) connected to the SWNT bundle, respectively, are shown at approximately 50 mK. This temperature is sufficiently below the critical temperature of 6.2 K of the Re electrodes, such that the superconducting state should be fully developed. As expected from the high room-temperature resistances, step-formation is observed, indicative of single-particle tunneling dominating the electrical transport through the device. From the data the charging energy for the tube can be estimated to be approximately 4 meV which is comparable to earlier reported values of 5.2 meV (Ref. 2) and 7 meV (Ref. 1) for SWNTs contacted under similar conditions with normal metal leads. In agreement with the above discussion, no peaks at the onset of steps are observed indicating that the SWNT is in a LL-like state.

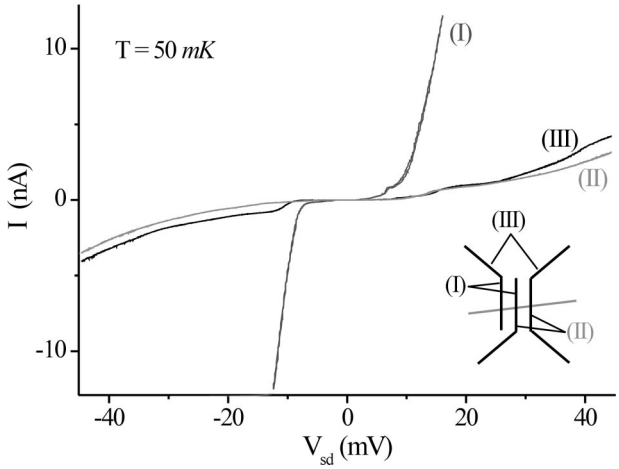

FIG. 3. Output characteristics of the three electrode pair configurations of Fig. 2. No peaks are observed at the onset of current-steps.

The dependence of the I/V_{sd} characteristics on the backgate-voltage V_g was qualitatively found to be the same for all three pairs of contacts, hence only the results for the pair of electrode (II) are shown in Fig. 4: for no V_g value is a gapless I/V_{sd} characteristic observed, as expected by the model discussed above [cf. Fig. 1(b)] which again indicates that the continuous line is indeed superconducting. At $|V_{\mathrm{sd}}|$ values $\gtrsim$15 mV current fluctuations are observed in some I/V_{sd} curves which are attributed to contact region instabilities versus time. In the region $|V_{\mathrm{sd}}|\lesssim15$ mV, for some (V_g,V_{sd}) values, weakly pronounced peaks are apparent at the onset of current steps. In the inset of Fig. 4 an enlarged view of one of the current-steps is shown.

In order to compare the experimental findings with the above presented theory, the product $\tau_{n+1}(\epsilon_{\mathrm{exc}})\cdot D_{\mathrm{QP}}[\mu(n+1;\{V_l\})-\mu_r+\epsilon_{\mathrm{exc}}]$ was explicitly calculated and used to determine I_{stat} through a superconductor/LL/superconductor (SC/LL/SC) system. The result for different values of γ (0.2, 0.25, and 0.3) are depicted in the inset of Fig. 5 together with

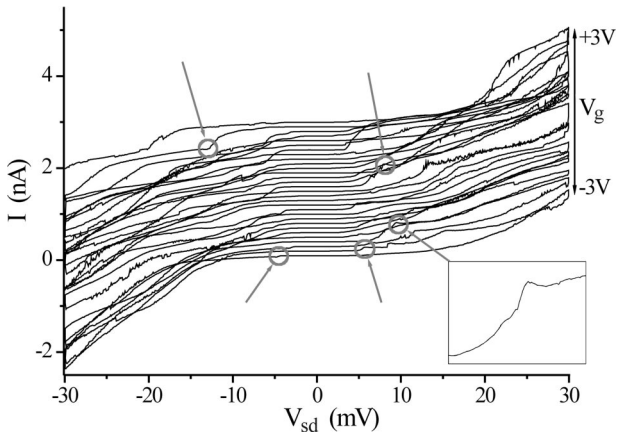

FIG. 4. Output characteristics of electrode pair (II) at backgate-voltages from -3 to $+3$ V in steps of 200 mV. At some backgate voltages weakly pronounced peaks (some are indicated by arrows and circles) are observed at the onset of a current step. Inset: enlarged view of one of the shallow peaks.

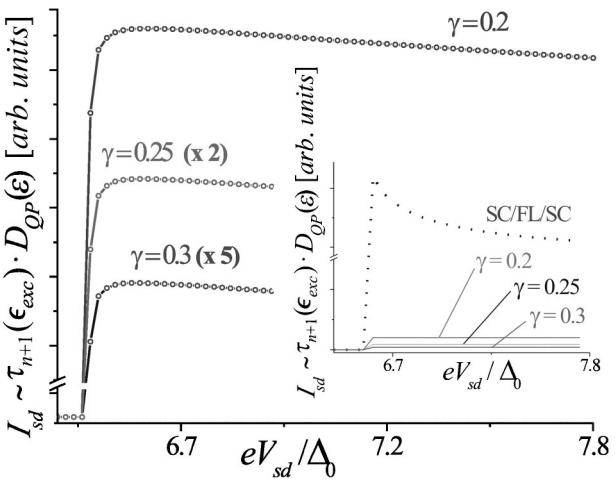

FIG. 5. Calculated shape of a current-step of a SC/LL/SC system for γ values of 0.2, 0.25, and 0.3 using the experimental values for the charging energy and the superconductor gap. The curves are shifted relatively towards each other for clarity and scaled by the factor indicated. A weak overshoot is observed on each of the curves. The overshot residues from the strongly developed peak due to the QP density of states in the superconductor in case the island in between is in a FL-like state (see the inset). Inset: the results for γ equal to 0.2, 0.25, and 0.3 and the curve for a SC/FL/SC configuration are depicted. The curves are not shifted to each other to stress the reduction of the overall current traversing the device. Clearly the suppression of the current peak (SC/FL/SC configuration) at the onset of the current step is observable in the curves where the island is in a LL-like state.

a calculated curve of a superconductor/Fermi liquid/superconductor (SC/FL/SC) configuration. Clearly a suppression of the current-peak at the onset of the SC/FL/SC system is observed compared to the SC/LL/SC system. A closer inspection of the onset of the curves (main Fig. 5, curves are shifted and scaled for clarity) reveals small overshots, which become less and less pronounced with increasing γ. Thus evidently, Fig. 5 shows, that current peaks originating from the QP density of states are not reduced completely; but a small overshot remains at the onset of each current step which is observed in the experimental data as weakly pronounced peak (cf. the inset Fig. 4).

Note that the mechanism leading to the suppression of QP tunneling induced current peaks is not affected in the event several SWNTs are connected in parallel to superconducting leads which might be possible in a SWNT rope or bundle. Also the formation of a currentless band of width $4\Delta(T)/e$ in the (V_{sd} vs V_g) plane is not altered by such a parallel contacting.

In summary, within a simple, qualitative model it could be demonstrated that in contrast to FL-like islands with weak electrical connection to superconducting leads, for a LL-like island its excitation spectrum leads to qualitative differences in the electrical transport. In the latter case, the energy dependence of the tunneling density of states of the LL-like island has to be taken explicitly into account. The tunneling density of states acts as a counterpart to the QP density of states in the superconducting leads. This results in a suppression of QP tunneling induced current peaks at the onset of each current step in the I/V_{sd} characteristics caused by an additional charge state becoming available for the island. The suppression is not necessarily complete as could be demonstrated by a theoretical simulation of a current step.

As SWNTs at low temperatures are assumed to be in a LL-like state, superconducting Re electrodes have been used to electrically weakly contact them in order to investigate whether the theoretically predicted effect is observable. Electrical transport measurements down to temperatures lower than 0.1 K were performed, showing the suppression of QP tunneling induced current peaks. Thus, these observations are consistent with the expectation of a LL-like state in SWNTs.

*Corresponding author. Email address: krstic@grenoble.cnrs.fr

[1] M. Bockrath, D. H. Cobden, P. L. McEuen, N. G. Chopra, A. Zettel, A. Thess, and R. E. Smalley, Science **275**, 1922 (1997).
[2] S. J. Tans, M. H. Devoret, H. Dai, A. Thess, R. E. Smalley, L. J. Geerligs, and C. Dekker, Nature (London) **386**, 474 (1997).
[3] L. I. Glazman, in *Single Electron Tunneling*, J. Low Temp. Phys. **118**, 247 (2000); A. N. Korotkov, in *Molecular Electronics* (Blackwell, Oxford, UK, 1997), p. 178.
[4] M. Bockrath, D. H. Cobden, J. Lu, A. G. Rinzler, R. E. Smalley, L. Balents, and P. L. McEuen, Nature (London) **397**, 598 (1999).
[5] C. Kane, L. Balents, and M. P. A. Fisher, Phys. Rev. Lett. **79**, 5086 (1997).
[6] C. Schönenberger, A. Bachthold, C. Strunk, J. P. Salvetat, and L. Forro, Appl. Phys. A: Mater. Sci. Process. **69**, 283 (1999).
[7] A. Y. Kasumov, R. Deblock, M. Kociak, B. Reulet, H. Bouchiat, I. I. Khodos, Y. B. Gorbatov, V. T. Volkov, C. Journet, and M. Burghard, Science **284**, 1508 (1999).
[8] J. Weis, R. J. Haug, K. v. Klitzing, and K. Ploog, Semicond. Sci. Technol. **9**, 1890 (1994).
[9] D. Pfannkuche, and S. E. Ulloa, *Advances in Solid State Physics*, edited by R. Helbig (Vieweg, Wiesbaden, Germany, 1996), Vol. 35, p. 65; D. Weinmann, W. Häusler, and B. Kramer, Ann. Phys. (Leipzig) **5**, 652 (1996).
[10] D. Weinmann, W. Häusler, W. Pfaff, B. Kramer, and U. Weiss, Europhys. Lett. **26**, 467 (1994).
[11] D. C. Ralph, C. T. Black, and M. Tinkham, Phys. Rev. Lett. **74**, 3241 (1995).
[12] C. B. Whan and T. P. Orlando, Phys. Rev. B **54**, R5255 (1996).
[13] V. Krstić, G. S. Düsberg, J. Muster, M. Burghard, and S. Roth, Chem. Mater. **10**, 2338 (1998).
[14] V. Krstić, S. Roth, and M. Burghard, Phys. Rev. B **62**, R16 353 (2000).
[15] *Supraleitende Werkstoffe*, edited by O. Henkel and E. M. Sawitzkij (VEB, Leipzig, 1982), p. 240.
[16] *Handbook of Chemistry and Physics*, 78th ed., edited by D. R. Lide (CRC Press, Boca Raton, FL, 1997), pp. 12–45.
[17] A. Rochefort, P. Avouris, F. Lesage, and D. R. Salahub, Phys. Rev. B **60**, 13 824 (1999).
[18] V. Krstić, J. Muster, G. S. Duesberg, G. Philipp, M. Burghard, and S. Roth, Synth. Met. **110**, 245 (2000).
[19] V. V. Schmidt, in *The Physics of Superconductors*, edited by P. Müller and A. V. Ustinov (Springer, Berlin, 1997).